

Error reduction of the Doppler lidar signal using a re-normalization method

NAK-GYU PARK¹, SUNG-HOON BAIK^{1*}, SEUNG-KYU PARK¹,
DONG-LYUL KIM¹, DUK-HYEON KIM²

¹Korea Atomic Energy Research Institute, 1045 Daedeokdaero, Yuseong-gu,
Daejeon 305-353, Republic of Korea

²Division of Cultural Studies, Hanbat National University, 16-1 Duckmyoung-Dong, Yuseong-gu,
Daejeon 305-719, Republic of Korea

*Corresponding author: shbaik@kaeri.re.kr

In this paper, we present a re-normalization method for a Doppler signal of a Doppler lidar system. For the Doppler lidar system, we used an injection-seeded pulsed Nd:YAG laser as a transmitter and an iodine cell as a Doppler frequency discriminator. A frequency locking system that uses the absorption feature of iodine gas is too sensitive to the external or internal noises (iodine cell temperature instability, laser frequency fluctuation, environmental noises, *etc.*) to maintain its locking point ideally, and this frequency locking error makes the Doppler lidar system acquire the noises as the Doppler frequency shifts. To reduce the Doppler signal error induced by a frequency locking error, we used a re-normalization method by an addition of a laser beam path separated from a transmitter to the Doppler frequency discriminator for re-normalization. In this method, fluctuations of the Doppler signal were reduced using the reference signal. The reduced amount of standard deviation between the Doppler signal and the re-normalization signal was 4.838×10^{-3} and the Doppler signals showed a 53.3% fluctuation reduction of the averaged error value by this method.

Keywords: injection-seeded laser, Doppler lidar, frequency locking, wind lidar, Doppler velocity measurement.

1. Introduction

A Doppler lidar [1–4] has been developed to provide wind measurements with high spatial and temporal resolution [5, 6], and the use of Doppler lidar technology to measure atmospheric winds has gained importance in atmospheric dynamics and weather forecasting based on numerical models [7].

According to the Doppler effect, velocities are derived from the transmission changes of backscattered light through a frequency discriminator [8].

Many researchers in the field of a Doppler lidar system use a molecular or atomic absorption discriminator (such as an iodine cell), which is used to calculate the amount of Doppler frequency shift and lock the frequency of the transmitter [9]. The use and

precise control of such equipment make a laser of a lidar system stable. However, there could be a fluctuation in the Doppler signal at a pulse-to-pulse or long-term region no matter how the equipment is used. The instability of the laser temperature control and a frequency locking algorithm, environmental noises, and unknown effects make the laser frequency unstable.

In this study, we propose a calibration method that can reduce the fluctuation of Doppler signals in a Doppler lidar system by using a reference signal from an additional laser beam path which is separated from the laser beam used for frequency locking process and located at an iodine cell. The reference signal is monitored and acquired by the lidar system controller. We apply incoherent Doppler wavelength discrimination to the Doppler lidar receiving system and evaluate the system's performance using a rotating disc.

2. Experimental setup for Doppler lidar system

2.1. Injection-seeded laser

A necessary condition of the laser in a Doppler lidar system is a narrow bandwidth. The bandwidth or line width of current commercially available unseeded Nd:YAG (532 nm) pulse lasers is about 30 GHz. We used the single longitudinal mode of a continuous wave seeder laser with a bandwidth of less than 10 kHz as the injection source to obtain a pulsed laser with a bandwidth of 100 MHz at 532 nm.

The laser system should also be tunable. The advantage of the seeder laser is the tunability and its tunable frequency range is very wide, such as 10 GHz at around 532 nm. The laser radiation power (3 mW) is also several orders of magnitude higher than that of spontaneous radiation in the resonance cavity. When the seeder laser frequency is tuned at the proper range of the iodine absorption lines, a Q-switched Nd:YAG laser pulse beam also develops at that frequency. The iodine cell for frequency locking and the lidar laser specifications are listed in Table 1.

2.2. Wavelength selection and calibration beam setup

In the case of the iodine Doppler lidar technique, the iodine vapor filter must be temperature controlled because the spectral absorption profiles depend on pressure and temperature. As we can see in Fig. 1, the transmittance property of the iodine cell is

Table 1. The iodine Doppler lidar system specifications.

	Parameter specification
Iodine cell	Length: 250 mm
	Diameter: 76 mm
	Thermocouple: type T
Laser	Seeder laser line width <10 kHz
	Bandwidth: 100 MHz
	Type: frequency-doubled pulsed

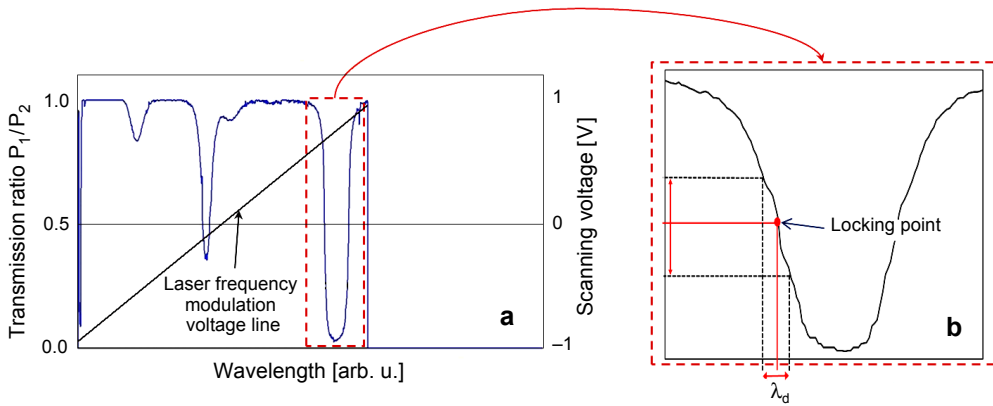


Fig. 1. The laser transmission ratio through the iodine cell against the tunable seeder-laser wavelength for external input voltages of -1 V to $+1$ V varied in steps of 100 μ V (a). The laser output at 532 nm is locked at a transmission ratio of 0.5 (b).

straightforward as expected from theory. To lock the laser frequency more precisely, we must choose the most sensitive area where the slope of the iodine gas' absorption line is the biggest in response to a small change in the laser frequency tuning voltage.

For the frequency locking process, we obtain the laser transmission ratio through the iodine cell as a function of the tunable seeder laser wavelength for external input voltages of -1 V to $+1$ V varied in steps of 100 μ V; the frequency tuning range of the laser is 0.87 MHz, and wavelength is locked at a transmission ratio point 0.5 . The mean squared error of the frequency locking process was 3.87 MHz, which corresponds to a wind velocity detection limit of approximately 1.04 m/s.

Figure 1 shows the plots of the transmission ratio through the iodine cell against the tunable seeder laser wavelength for external input voltage changes. Our frequency locking system can control the locking point for fluctuations by 1% , but small variances in the wavelength of the laser frequency from external noises can make a big difference in the transmission ratio and produce an error in the Doppler frequency shift.

A schematic diagram of the configured Doppler lidar system is shown in Fig. 2. We divide the injection-seeded Nd:YAG laser beam into two separate beams using a beam splitter (BS1). The transmitted beam is sent to a rotating metallic plate, whereas the reflected beam is transmitted to a frequency locking system through an optical fiber. The transmitted laser lights are scattered from the rotating disc with an adjusted rotating speed. The speed of the rotating disc can be determined from the Doppler receiving system and an improvised encoder. The Doppler-shifted scattered light is collected in the backward direction and transmitted through the optical fiber. Subsequently, the light is divided into two channels. One (reference) channel detects the scattered light directly, whereas the other channel detects the transmitted light that passes through an iodine cell.

For frequency locking equipment, we divide the laser light reflected on BS1 using BS3 before it is transmitted through the target iodine cell. The reflected light signal is

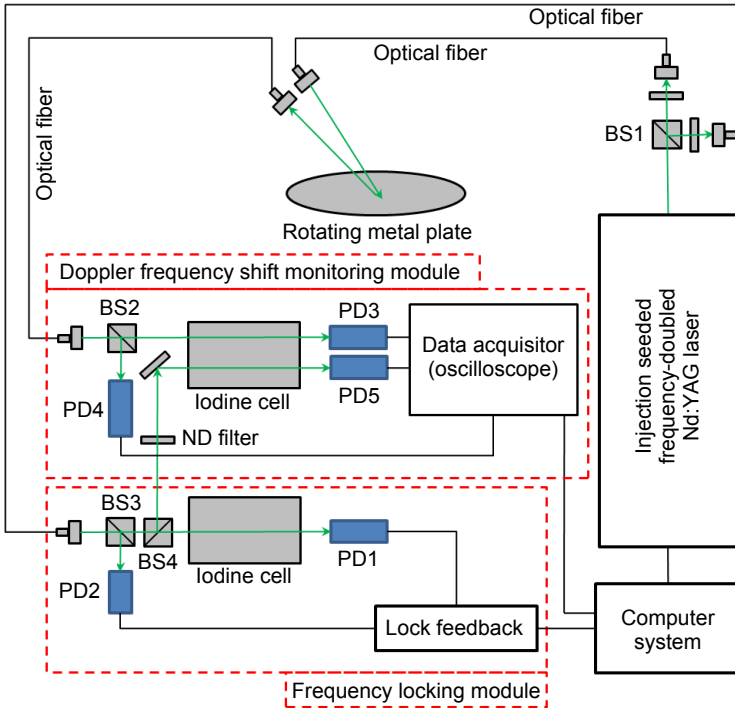


Fig. 2. Schematic diagram of the configured Doppler lidar system.

acquired by photodiode (PD2), and this signal is used to compensate the pulse-energy fluctuation of the seeded laser. The transmitted light is divided using BS4. One path is used for monitoring the frequency shift by PD1, and the other path is used for calibrating the Doppler signals by PD5. When the laser frequency modulating voltages are impressed from -1 V to $+1$ V, the reflected laser beam intensity (PD2) is not varied but the transmitted laser beam intensity (PD1) is varied with laser frequencies on account of iodine gas' absorption feature. Therefore the ratio variation of PD1 signal to PD2 signal shows the relative frequency shift of the laser. The ratio was locked to 0.5 by using the lock feedback equipment as shown in Fig. 1b. If the laser lights scattered from the rotating disc have Doppler frequency shifts, the ratio of PD3 signal to PD4 signal will be varied with the velocity of the rotating disc. As this ratio (Doppler signal) can be unstable owing to various noises as shown in Fig. 3, the reflected laser beam from BS4 was used for re-normalization. The signals of PD3, PD4 and PD5 were acquired by an oscilloscope. These ratios were displayed on a monitor and the computer system saved the acquired data. We used two identically modeled iodine cells with the same conditions (set temperature 60 °C) for frequency locking and monitoring of Doppler frequency shift as shown in Table 1. We used large size photodiodes (SM1PD1A, Thorlabs) for frequency locking (PD1, PD2). A frequency locking program and a sample and holder system have been developed. There was little space in

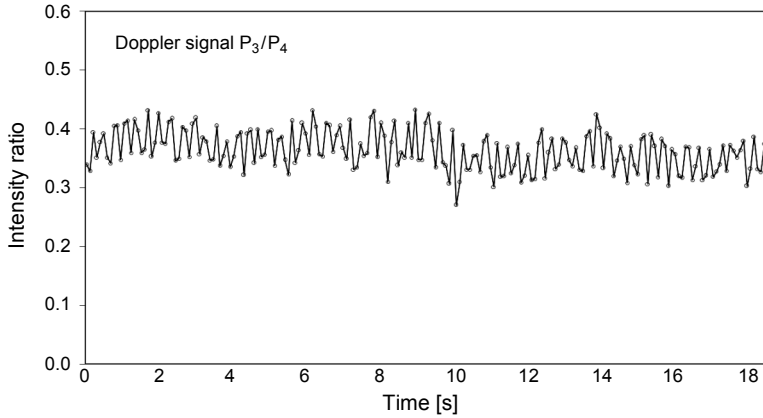


Fig. 3. Raw Doppler signal.

one iodine cell for another photodiode. If there is available space for another photodiode and the system configuration is possible to use single iodine cell, we could acquire experimental results with less noise.

2.3. Experimental results

The rotating plate stopped for about 8 s and accelerated for a few seconds. Then, the rotating plate was maintained at the same velocity. We acquired the signal of PD3 and PD4 for 18 s. As shown in Fig. 3, the fluctuation of the Doppler signal was so big in entire rotating conditions that we could not even discriminate the rotating state of the plate, *i.e.*, we could not see whether the plate was moving or not.

Figure 4 shows the Doppler signal S_D and reference signal S_R for re-normalization for 3 s. The fluctuation of the Doppler signal has a similar periodic shape with the ref-

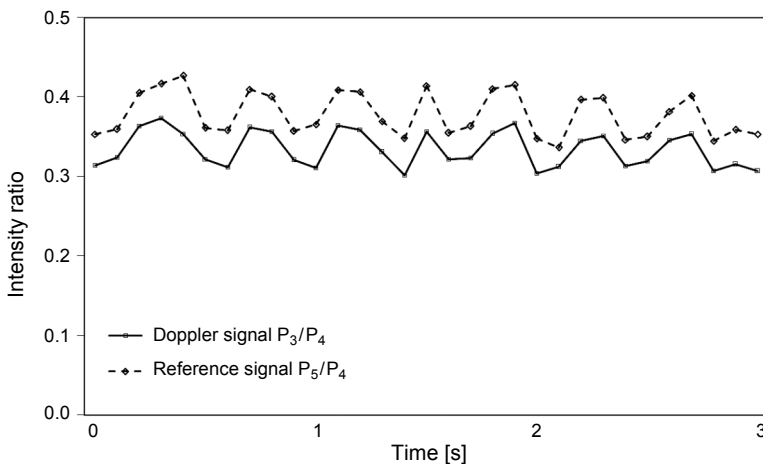


Fig. 4. Raw Doppler signal and reference signal in pulse to pulse (short-term fluctuation).

erence signal excluding their absolute ratio. We therefore used this similarity for re-normalizing a Doppler signal.

$$S_D = P_3/P_4 \quad (1)$$

$$S_R = P_5/P_4 \quad (2)$$

where S_D and S_R are the intensity ratio of the Doppler signal and the reference signal, respectively, P_3 , P_4 and P_5 are the output voltage of photodiode 3, 4 and 5, respectively. The data processing for the acquired signals is conducted by 10 Hz which is the same with a laser repetition rate. Reference signal S_R is used to compensate the frequency locking error induced by the laser intensity fluctuation.

In order to reduce the fluctuations of raw signals, we filtered both signals. All measurements were averaged by 30 pulses for 18 s. The results of which are shown in Fig. 5. As shown in Fig. 5, we not only discriminate the acceleration state in which the velocity of the plate is accelerated specifically, but also the stationary and rotational state. However, these results are insufficient for use as data in a Doppler lidar system because the signal has low frequency fluctuations in the same state of the rotating plate. In terms of the velocity measurement system, these fluctuations are system noise or errors mainly due to a frequency locking error.

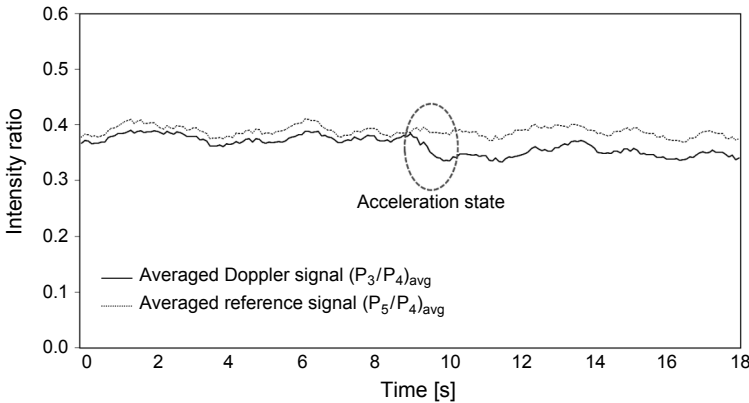


Fig. 5. Averaged Doppler signal and reference signal (long-term fluctuations).

If we look at the Doppler signal line and the reference signal line closely enough, we can see that they have a similarity in the sloshing period. We therefore used a reference signal ratio from photodiodes 4 and 5 as a re-normalization factor.

$$S_{\text{re-no (a)}} = \frac{(P_3/P_4)_{\text{avg}}}{\alpha(P_5/P_4)_{\text{avg}}} \frac{1}{\text{offset}_{(a)}} \quad (3)$$

$$S_{\text{re-no (b)}} = (P_3/P_4)_{\text{avg}} - \alpha(P_5/P_4)_{\text{avg}} + \text{offset}_{(b)} \quad (4)$$

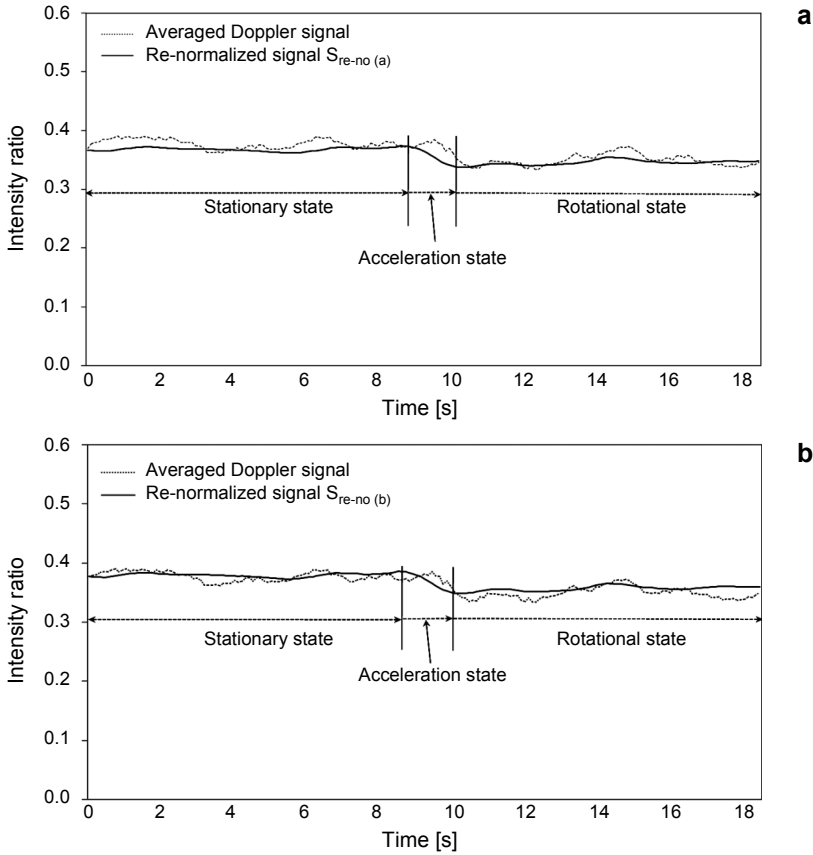


Fig. 6. Re-normalized Doppler signal to use the ratio of the Doppler signal and reference signal (a), and the difference in the Doppler signal and reference signal (b).

where S_{re-no} is the re-normalized signal and $(P_3/P_4)_{avg}$, $(P_5/P_4)_{avg}$ are the averaged values of S_D and S_R , respectively, α is the normalization factor adjusted by a ND filter.

The signal re-normalized by using Eqs. (3) and (4) is shown in Fig. 6. The fluctuations in the re-normalized signal were much smaller than those of the averaged Doppler signal for the entire area in both ways: the use of the ratio (Eq. (3)) and of the difference (Eq. (4)).

We measured the varied velocities of a rotating plate by applying this method, the experimental results of which are shown in Fig. 7. The applied velocities were: -15 , -10 , -5 , $+5$, $+10$, $+15$, $+20$, $+25$, $+30$ and $+35$ m/s. The values of y-axis are the variances of intensity ratios between the stationary state and the rotational state in the respective velocity of the rotating plate. These variances can be converted into velocities of the target plate and the measured values are proportional to the velocities of the rotating plate.

Table 2 shows the averaged standard deviations of the averaged Doppler signal and re-normalized signal. We sampled 50 measurements of the same area at the applied

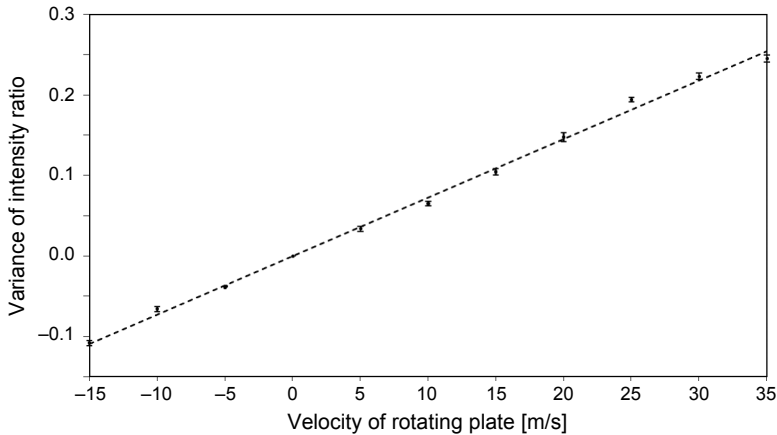


Fig. 7. Plot of changes in the re-normalized signal against the actual velocities of the rotating plate.

Table 2. Standard deviations of the averaged signal and the re-normalized signal.

Standard deviation (averaged values for all of the applied velocities)		
The averaged Doppler signal	The re-normalized signal	The reduced amount
9.085×10^{-3}	4.247×10^{-3}	4.838×10^{-3}

velocities. As shown in Table 2, the reduced amount of standard deviation between the Doppler signal and re-normalization signal was 4.838×10^{-3} from 9.085×10^{-3} to 4.247×10^{-3} , and all of the applied signals showed a 53.3% fluctuation reduction of the averaged error value.

3. Conclusions

In this paper, we presented a re-normalization method for the fluctuations of Doppler signals from the various noises mainly due to the frequency locking error for a Doppler lidar system. For the Doppler lidar system, we used an injection-seeded pulsed Nd:YAG laser as a transmitter and an iodine filter as a Doppler frequency discriminator. For the Doppler frequency shift measurement, the transmission ratio using the injection-seeded laser is locked to stabilize the frequency. If the frequency locking system is not perfect, the Doppler signal has some error due to the frequency locking error. The re-normalization process of the Doppler signals was performed to reduce this error using an additional laser beam to an iodine cell. We confirmed that the re-normalized Doppler signal shows the stable experimental data much more than those of the averaged Doppler signal using our calibration method, the reduced standard deviation was 4.838×10^{-3} .

We have a plan to perform atmospheric measurements in the future.

Acknowledgements – This work was supported by the National Research Foundation of Korea (NRF), grant funded by the Ministry of Science, ICT and Future Planning (No. 2012M2A84055613).

References

- [1] FRIEDMAN J.S., TEPLY C.A., CASTLEBERG P.A., ROE H., *Middle-atmospheric Doppler lidar using an iodine-vapor edge filter*, Optics Letters **22**(21), 1997, pp. 1648–1650.
- [2] MCKAY J.A., *Assessment of a multibeam Fizeau wedge interferometer for Doppler wind lidar*, Applied Optics **41**(9), 2002, pp. 1760–1767.
- [3] CHIAO-YAO SHE, JIA YUE, ZHAO-AI YAN, HAIR J.W., JIN-JIA GUO, SONG-HUA WU, ZHI-SHEN LIU, *Direct detection Doppler wind measurements with a Cabannes–Mie lidar: A. Comparison between iodine vapor filter and Fabry–Perot interferometer methods*, Applied Optics **46**(20), 2007, pp. 4434–4443.
- [4] CHIAO-YAO SHE, JIA YUE, ZHAO-AI YAN, HAIR J.W., JIN-JIA GUO, SONG-HUA WU, ZHI-SHEN LIU, *Direct-detection Doppler wind measurements with a Cabannes–Mie lidar: B. Impact of aerosol variation on iodine vapor filter methods*, Applied Optics **46**(20), 2007, pp. 4444–4454.
- [5] LEI TANG, ZHIFENG SHU, JIHUI DONG, GUOCHENG WANG, YONGTAO WANG, WENJING XU, DONGDONG HU, TINGDI CHEN, XIANKANG DOU, DONGSONG SUN, HYUNKI CHA, *Mobile Rayleigh Doppler wind lidar based on double-edge technique*, Chinese Optics Letters **8**(8), 2010, pp. 726–731.
- [6] LIU Z.S., LIU B.Y., LI Z.G., YAN Z.A., WU S.H., SUN Z.B., *Wind measurements with incoherent Doppler lidar based on iodine filters at night and day*, Applied Physics B **88**(2), 2007, pp. 327–335.
- [7] MENZIES R.T., *Doppler lidar atmospheric wind sensor: a comparative performance evaluation for global measurement application from earth orbit*, Applied Optics **25**(15), 1986, pp. 2546–2553.
- [8] LI F.Q., CHENG X.W., LIN X., YANG Y., WU K.J., LIU Y.J., GONG S.S., SONG S.L., *A Doppler lidar with atomic Faraday devices frequency stabilization and discrimination*, Optics and Laser Technology **44**(6), 2012, pp. 1982–1986.
- [9] SUNGCHUL CHOI, SUNGHOON BAIK, SEUNGKYU PARK, IMKANG SONG, DUKHYEON KIM, JINMAN JUNG, *Development of single-filter Doppler signal discrimination method for incoherent Doppler lidar system*, Optica Applicata **42**(3), 2012, pp. 545–553.

*Received October 17, 2013
in revised form January 16, 2014*